Advances in D-bar methods for partial boundary data electrical impedance tomography

—

From continuum to electrode models and back

Andreas Hauptmann

Academic dissertation

To be presented for public examination with the permission of the Faculty of Science of the University of Helsinki in Sali 13 in the main building (Fabianinkatu 33, Helsinki) on 30th June 2017 at 12 o'clock.

Department of Mathematics and Statistics
Faculty of Science
University of Helsinki

HELSINKI 2017

ISBN 978-951-51-3497-4 (paperback)
ISBN 978-951-51-3498-1 (PDF)

http://ethesis.helsinki.fi

Unigrafia Oy
Helsinki 2017

Acknowledgements

First and foremost I want to express my deepest gratitude to my advisor Samuli Siltanen, who supported and guided me throughout the years since my time as exchange student at the University of Helsinki in 2011. We were certainly never short of scientifically intriguing projects to work on, which lead me to discover electrical impedance tomography as a challenging problem for my thesis. Thank you for being a great mentor, scientifically and personally.

I would also like to thank my former colleagues at AJAT, where I have spent my first two years during my PhD studies as R&D Scientist. I have learned so many lessons from real world applications that will be highly valuable for my future as an application driven computational mathematician. Personally I want to thank my team leader Henrik Lohman, our group leader Tuomas Pantsar, and our former CEO Konstantinos Spartiotis for inspiring discussions, as well as Annette Onodera for the important non-technical conversations.

I wish to cordially thank my pre-examiners Nuutti Hyvönen and Jennifer Mueller, as well as my opponent David Isaacson for their valuable time spent reading my thesis.

Furthermore I acknowledge the immense impact my collaborators had on my scientific development. I am thankful for the time Sarah Hamilton invested during her postdoc in Helsinki to explain the D-bar algorithm to a young and confused PhD student; Matteo Santacesaria for our great synergy of theoretical and computational expertise; Melody Alsaker for her valuable understanding of the a-priori method.

Thanks to Tapio Helin I had the opportunity to work on a fascinating project with the Inverse Problems group at the University of Münster on dynamic X-ray tomography, additionally to my studies on electrical impedance tomography. I especially thank Martin Burger for the hospitality in Münster, as well as Lena Frerking and Hendrik Dirks for a great project and the nice running routes.

An important aspect for the success of my thesis is certainly my full time at the University of Helsinki, for which I thank Gunther Uhlmann, Matti Lassas, and the Academy of Finland for providing the needed funding. I am happy that I had with Paola Elefante such a nice office mate, as well as my great colleagues Hanne Kekkonen, Teemu Saksala, Tatiana Bubba, and Jonatan Lehtonen, that I frequently disturbed when I was stuck. I also enjoyed our lunch discussions with my colleagues Zenith Purisha, Minh Mach, Jussi Korpela, and Antti Kujanpää. The Department of Mathematics and Statistics earned a big thank you for the coffee supply that certainly helped this work to advance.

On a not so scientific level, but immensely important for my mental health have

been my friends in Helsinki, most importantly General Nonsense, that helped me trough the harder times as well as making the good ones even better. On a broader level I thank Hämäläis-Osakunta for making me feel home away from my birth country and especially Koivuniemi for the unforgettable summer days, sunsets and early sunrises. But also my friends Alexander Pachonik and Christian Denk in Germany deserve a thank you for a long friendship that always feels like back in the days. I am also thankful for the frequent visits from Verena Mimm and the time we spent exploring Helsinki's restaurants.

My parents, Monika Hauptmann and Ralf Hauptmann, certainly have a big part in making this work happen, by supporting me throughout my life. Regardless of my decisions I was always able to count on their full support, leading to the independent person I am now.

Lastly, I thank Maria Kekäläinen for a few wonderful years in Helsinki, making the place I chose for living a real home.

Helsinki, June 2017

Andreas Hauptmann

The thesis consists of this overview and the following articles:

List of Publications

[I] S. Hamilton, A. Hauptmann, and S. Siltanen, *A Data-Driven Edge-Preserving D-bar Method for Electrical Impedance Tomography,* Inverse Problems and Imaging, 8(4), pp. 1053–1072, 2014.

[II] A. Hauptmann, S. Santacesaria, S. Siltanen, *Direct inversion from partial-boundary data in electrical impedance tomography,* Inverse Problems, 33(2), 025009, 2017.

[III] M. Alsaker, S. Hamilton, and A. Hauptmann, *A Direct D-bar Method for Partial Boundary Data Electrical Impedance Tomography with A Priori Information,* Inverse Problems and Imaging, 11(3), pp. 427–454, 2017.

[IV] A. Hauptmann, *Approximation of full-boundary data from partial-boundary electrode measurements,* arXiv:1703.05550.

Author's contribution

[I] Crucial parts in developing the algorithm are due to the author and all computational studies are conducted by the author. Writing has been done in equal parts.

[II] The theoretical development is due to the author. Computations are conducted by the author and major parts of writing.

[III] The theoretical background, computations, and writing is done in equal parts with the other authors.

[IV] Analysis, computations, and writing is done in its entirety by the author.

Contents

1 Introduction

Seeing inside an object or to determine the cause of phenomena has been the driving question of scientific research for centuries. However mathematics was for a long time concerned with the question of how to model the observation process, the so called *forward problem*. This tradition has changed, when mathematicians started to ask how to determine the cause from its observation and a new branch of so-called *inverse problems* was born. These problems are typically ill-posed, which means given some data there might be no solution, no unique solution, or no continuous dependence between solutions and data. Thus, only a few ambitious mathematicians, such as E. Fredholm, J. Radon, and A. Tikhonov, started to investigate these challenging problems in the early 20th century. Later the computational era has sparked new interest in inverse problems research and many scientists from other fields than mathematics joined the quest for the unknown cause.

One branch of inverse problems that has especially drawn interest are tomographic imaging methods, where one wants to see inside a physical body without invading it. Measurements are conducted from the outside and slices (Greek: $\tau o \mu os$) are being reconstructed from the obtained information. Among these tomographic methods, medical imaging modalities had the biggest impact on our society by enabling physicians to see inside the human body without surgery or other invasive methods. Most notably Allan M. Cormack and Godfrey N. Hounsfield were awarded *The Nobel Prize in Physiology or Medicine 1979* for their development of computer assisted tomography [17], which is nowadays commonly referred to as *computerized tomography* (CT). Mathematically, their work can be seen as an implementation of Johann Radon's early study *"On the determination of functions from their integral values along certain manifolds"*[1] [59], even though Cormack and Hounsfield had apparently no knowledge of Radon's work. This particular example illustrates the importance of combining theoretical and solid mathematical work with an application driven attitude. Especially in computational mathematics it is important to keep the application in mind.

In particular we are in this thesis interested in a rather new approach to medical imaging that is motivated by using electricity to determine the inside of a body. The clear advantage lies in the usage of harmless electric currents, in contrast to the ionizing radiation of X-rays, whereas the mathematical problem is inherently more challenging. This imaging modality is commonly referred to as *electrical impedance tomography* (EIT) and seeks to reconstruct an image of the inner organs by de-

[1] Published originally in German as *"Über die Bestimmung von Funktionen durch ihre Integralwerte längs gewisser Mannigfaltigkeiten"*.

termining their conductivity, i.e. how well electricity is conducted. As a medical imaging modality it is most promising in pulmonary and cardiac imaging, due to considerably different conductivity values in the air filled lungs (low conductive) and the blood filled heart (high conductive). EIT is in principle capable of monitoring the respiratory process, detecting pathologies in the lungs, and monitoring the heart activity.

The main focus of this work is on the partial-boundary problem in EIT, that means one has only access to a certain part of the boundary and data can only be collected there. In a hospital setting these situations can arise when monitoring a critical or unconscious patient and hence one can only access the front of the torso (ventral position). Furthermore, practical complications can arise due to faulty, dislocated, or dispatched electrodes and hence leading to incomplete data. The methods presented in this thesis are capable of dealing with such incomplete data. Following the tradition of mathematical research we are also interested in quantifying the error incomplete data introduces to the reconstruction.

In a short summary, this thesis investigates how to improve EIT reconstructions from partial-boundary data by utilizing concepts from an ideal mathematical setting as well as how to apply these methods to real electrode models and measurement data. This introductory part is oraganized as follows. At first we discuss the ideal mathematical background in Section 2, with an overview of previous results and important contributions to the field. In the following Section 3 we will particularly discuss the partial-boundary problem and important differences between the ideal mathematical setting and real life applications. Followed by a discussion of measurement models in Section 4 and how to obtain the needed data in each case. Section 5 presents a short discussion of the results in each publication.

2 The inverse conductivity problem

In *electrical impedance tomography* (EIT) one wants to determine the conductivity distribution inside the measured object from electrical measurements at the boundary. The conductivity describes how well an object can conduct electricity and hence behaves inversely proportional to its resistance. Knowing the conductivity distribution inside an object is then equivalent to knowing important information of its structure.

To determine the conductivity with EIT, one typically injects a current through electrodes on the boundary and measures the resulting voltage distribution at the same electrodes. A typical experimental setup for such a system is shown in Figure 1. In this section we will first discuss the ideal mathematical setting for EIT as well

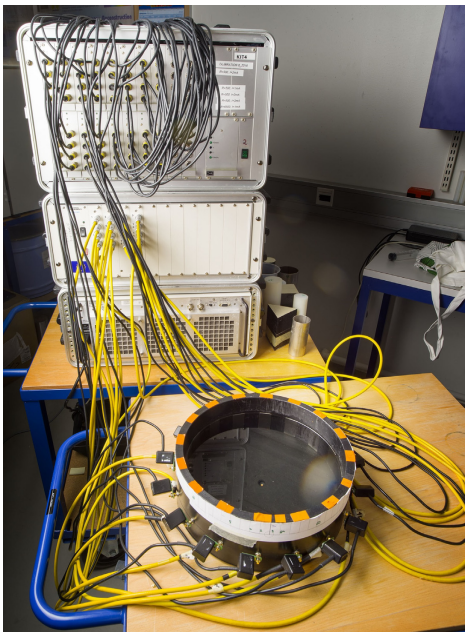

Figure 1: The KIT4 (Kuopio Impedance Tomograph 4) measurement system at the University of Eastern Finland, Kuopio. (Picture Courtesy: Samuli Siltanen)

as theoretical questions that were asked and mostly solved since the problem was first published in 1980 by Alberto Calderón.

2.1 Calderón's problem

In his classical seminar paper [11] Calderón stated the conductivity equation and asked whether one can determine the conductivity inside the domain from electrical measurements at the boundary. Mathematically speaking, given a bounded domain $\Omega \subset \mathbb{R}^n$, $n \geq 2$, with Lipschitzian boundary $\partial\Omega$, and let the conductivity σ be a real and measurable function with lower positive bound, then the conductivity equation is given by

$$\begin{aligned} \nabla \cdot \sigma \nabla u &= 0, \qquad \text{in } \Omega, \\ u|_{\partial\Omega} &= \varphi, \qquad \text{on } \partial\Omega\,. \end{aligned} \tag{1}$$

The Dirichlet boundary value is assumed to be known, corresponding to the voltage distribution on the boundary, whereas the Neumann data is measured, i.e. the current through the boundary. The infinite-precision voltage and current measurements

are modeled by the *Dirichlet-to-Neumann* (DN), or voltage-to-current, map

$$\Lambda_\sigma : \varphi \mapsto \sigma \frac{\partial u}{\partial \nu}\bigg|_{\partial\Omega}.$$

The inverse problem of determining the conductivity from the complete knowledge of the Dirichlet-to-Neumann map is known as the classical Calderón's problem. Calderón also published a first uniqueness result in his paper, where he assumed that σ is a constant plus a small perturbation δ, such that $\sigma(x) = 1 + \delta(x)$ for $x \in \Omega$. Under these assumptions he was able to show that the conductivity is uniquely determined by the boundary data.

Even though the inverse conductivity problem can be stated in a simple way, its solution needs a thorough mathematical understanding. The first global uniqueness result was published by Sylvester and Uhlmann in 1987 [64] for dimension $n \geq 3$ and smooth conductivities. For dimension $n = 2$ the problem is much harder to solve, since it is not overdetermined anymore. This can be seen from the Schwartz kernel of the DN map which has $2(n-1)$ degrees of freedom, from which we seek to determine the conductivity σ of n variables. Thus, in two dimensions all the information needs to be used and it took 10 additional years until a global uniqueness result was published by Nachman in 1996 [57] for twice differentiable conductivities $\sigma \in W^{2,p}(\Omega)$ and $p > 1$, based on earlier work in [56, 58]. Following research concentrated on reducing regularity assumptions on the conductivity; first to $\sigma \in W^{1,p}(\Omega)$ for $p > 2$ by Brown and Uhlmann [9], and then eventually to bounded and measurable conductivities $\sigma \in L^\infty(\Omega)$ by Astala and Päivärinta [5]. All of the aforementioned results are based on so-called *complex geometrical optics* (CGO) solutions and hence we will discuss the concept in the following. We will introduce one specific family of CGO solutions, based on the results in [57], that are important for our reconstruction procedure.

2.2 Complex geometrical optics solutions

The concept of complex geometrical optics solutions has been introduced as complex-valued functions that are solutions of a Schrödinger equation and have exponential growth in certain directions and exponential decay in others. They were first introduced by Faddeev in 1966 [21] and then later rediscovered as powerful tool in inverse problems by [7, 54, 63, 64]. We will introduce the concept here by an explicit example used in the proof by Nachman [57], since these are the CGO solutions utilized in this thesis. We will give the basic notation and ideas, for all rigorous technical details see the original articles [21, 57] and the summary in [51, 60].

Definition 2.1 (A class of complex geometrical optics solutions)
Let $q \in L^p(\mathbb{R}^2)$, $1 < p < 2$, then we define $\psi(z,k)$, for $z \in \mathbb{R}^2$ and $k \in \mathbb{C}\backslash\{0\}$, as solutions of the Schrödinger-type equation

$$(-\Delta + q)\psi(\cdot, k) = 0, \tag{2}$$

that satisfy the asymptotic condition

$$e^{-ikz}\psi(z,k) - 1 \in W^{1,\widetilde{p}}(\mathbb{R}^2), \quad \textit{with} \quad 2 < \widetilde{p} < \infty. \tag{3}$$

It was shown in [57] that there is a unique ψ for any $k \in \mathbb{C}\backslash\{0\}$ satisfying (2) and (3). Next we will introduce an important class of related CGO solutions, but let us first define a crucial operator for derivatives with respect to complex variables.

Definition 2.2 (The ∂_z operator)
Given the complex variable $z = x + iy$, we define

$$\partial_z := \frac{1}{2}\left(\frac{\partial}{\partial x} - i\frac{\partial}{\partial y}\right), \quad \textit{and} \quad \overline{\partial}_z := \frac{1}{2}\left(\frac{\partial}{\partial x} - i\frac{\partial}{\partial y}\right).$$

An important property of the $\overline{\partial}$ operator is given by its relation to the Cauchy-Riemann equations, which state that a function $f(z,\overline{z})$ is analytic if $\overline{\partial}_z f = 0$. Furthermore it is easy to see that the Laplacian $\Delta = \partial_{xx} + \partial_{yy}$ can be written as $\Delta = 4\,\overline{\partial}_z\,\partial_z$.

Now we can define a related class of CGO solutions that are important for the reconstruction. We set $\mu(z,k) := e^{-ikz}\psi(z,k)$ and immediately note by the property (3) that μ is in fact bounded. Inserting μ into (2) and noting that $\partial_z e^{ikz} = ike^{ikz}$ and $\overline{\partial}_z\, e^{ikz} = 0$, we obtain

$$\begin{aligned} q(z)e^{ikz}\mu(z,k) &= \Delta(e^{ikz}\mu(z,k)) \\ &= 4\partial\,\overline{\partial}(e^{ikz}\mu(z,k)) \\ &= 4(ike^{ikz}\,\overline{\partial}\,\mu(z,k) + e^{ikz}\partial\,\overline{\partial}\,\mu(z,k)) \\ &= e^{ikz}(4ik\,\overline{\partial} + \Delta)\mu(z,k). \end{aligned}$$

Thus, we obtain a partial differential equation for $\mu(z,k)$ as

$$(-\Delta - 4ik\,\overline{\partial}_z + q(z))\mu(z,k) = 0. \tag{4}$$

From this we aim to formulate an integral equation to compute μ, for which we need to introduce a special Green's function.

Definition 2.3 (Faddeev's Green's function)
Let $g_k \in L^{p'}(\mathbb{R}^2)$, for $1/p' + 1/p = 1$ and $1 < p < 2$, be the fundamental solution to

$$(-\Delta - 4ik\,\overline{\partial}_z)g_k(z) = \delta(z). \tag{5}$$

Then Faddeev's Green's function is defined by

$$G_k(z) := e^{ikz} g_k(z). \tag{6}$$

It can be easily seen that G_k is a Green's function for the Laplacian, since by definition follows

$$\begin{aligned} -\Delta G_k(z) &= -4\,\overline{\partial}_z\,\partial_z(e^{ikz}g_k(z)) \\ &= e^{ikz}(-4\,\overline{\partial}_z\,\partial_z g_k(z) - 4ik\,\overline{\partial}_z\,g_k(z)) \\ &= e^{ikz}(-\Delta - 4ik\,\overline{\partial}_z)g_k(z) \\ &= \delta(z). \end{aligned}$$

An important property of g_k is given by its symmetry

$$g_k(z) = g_1(kz),$$

where g_1 can be written with the exponential-integral function

$$g_1(z) = -\frac{1}{4\pi}e^{-iz}(\mathrm{Ei}(iz) + \mathrm{Ei}(-i\bar{z})) = -\frac{1}{2\pi}e^{-iz}\mathrm{Re}(\mathrm{Ei}(iz)),$$

as introduced in [8]. Most importantly, this function can be easily evaluated with modern scientific computing software.

By using Faddeev's Green's function, we are able to express $\mu(z,k)$ by a Lippmann-Schwinger-type equation

$$\mu(z,k) = 1 - (g_k * (q\mu(\cdot,k))(z), \tag{7}$$

or in its integral form

$$\mu(z,k) = 1 - \int_{\mathbb{R}^2} g_k(z-\zeta)q(z)\mu(z,k)\; d\zeta. \tag{8}$$

It is easy to see that (8) is a Fredholm integral equation of the second kind. Applying $-\Delta - 4ik\,\overline{\partial}$ to (7), shows that solutions of (7) are also solutions of (4). We conclude this chapter with the Lippmann-Schwinger-type equation for the CGO solutions ψ, by applying e^{ikz} to both sides in (7) we obtain

$$\psi(z,k) = e^{ikz} - (G_k * (q\psi(\cdot,k))(z), \tag{9}$$

which turns out to be the starting point of the reconstruction procedure described in the following section.

2.3 The classical D-bar method

From a computational point of view the most important part of Nachman's uniqueness proof is its constructiveness that means it outlined a reconstruction procedure to obtain the conductivity. The basic step is to transform the conductivity equation (1) into a Schrödinger equation and utilize the CGO solutions discussed in Section 2.2. For this purpose let $\Omega \subset \mathbb{R}^2$ be a bounded, simply connected, Lipschitz domain. The transformation is done by substituting $\tilde{u} = \sqrt{\sigma}u$, setting $q = \frac{\Delta\sqrt{\sigma}}{\sqrt{\sigma}}$ and extending $\sigma \equiv 1$ outside Ω. Then we get

$$(-\Delta + q(z))\tilde{u}(z) = 0 \qquad \text{for } z \in \mathbb{R}^2. \tag{10}$$

Due to the transformation some assumptions on the conductivity are needed. At first we need $\sigma \in C^2(\Omega)$ and $0 < c < \sigma(z)$ for $z \in \Omega$ such that the definition of q makes sense. For the extension we need that $\sigma(z) \equiv 1$ in a neighborhood of the boundary $\partial\Omega$.

The connection of (10) to the CGO solutions defined in (2) should be clear by now and the basic idea can be summarized as obtaining the function $\mu(z,k) = e^{-ikz}\psi(z,k)$ such that

$$\lim_{k\to 0} \mu(z,k) = \sqrt{\sigma(z)}, \qquad \text{for } z \in \Omega. \tag{11}$$

The above identity can be verified by taking the limit in (4) and with some special care on the singularity of g_k at $k = 0$. Anyhow, in practice one can just substitute $k = 0$ in (11) by the analysis in [6, 46] and compute the conductivity by

$$\mu(z,0) = \sqrt{\sigma(z)}.$$

Let us now discuss how to obtain μ from the measurements. The key here is the name-giving D-bar equation that is obtained by taking the $\overline{\partial}$ derivative with respect to k in (7) and one obtains (after careful analysis)

$$\overline{\partial}_k \mu(z,k) = \frac{1}{4\pi\bar{k}}\mathbf{t}(k)e_{-k}(z)\overline{\mu(z,k)}, \tag{12}$$

with the modified exponential $e_k(z) = e^{i(kz+\bar{k}\bar{z})}$ and the crucial scattering transform $\mathbf{t}(k)$ defined by

$$\mathbf{t}(k) := \int_{\mathbb{R}^2} e^{i\bar{k}\bar{z}} q(z)\psi(z,k)dz. \tag{13}$$

Thus, to solve the D-bar equation we need to obtain the scattering transform and this is where the DN map comes into the play. However, before we can do that, we need to state a crucial identity.

Theorem 2.4 (Alessandrini's identity [1])
Given a Dirichlet boundary value $f \in H^{1/2}(\partial\Omega)$, then for any two solutions $v_l \in H^1(\Omega),\ l = 1, 2$ to

$$(-\Delta + q_l)v_l = 0 \quad in\ \Omega, \quad v|_{\partial\Omega} = \varphi, \tag{14}$$

the following identity holds:

$$\int_\Omega (q_1 - q_2)v_1 v_2 dz = \int_{\partial\Omega} v_1(\Lambda_{q_1} - \Lambda_{q_2})v_2 ds. \tag{15}$$

Alessandrini's identity is given for the potentials q and hence before we can make use of it we need to establish the relation to our EIT data Λ_σ. We remind that the potential was defined by $q = \frac{\Delta\sqrt{\sigma}}{\sqrt{\sigma}}$. Let u be a solution of the conductivity equation (1) with the Dirichlet boundary value φ and let $v = \sqrt{\sigma}u$ be a solution of (14). Then it holds that

$$\Lambda_q\varphi = \sigma^{-1/2}\left(\Lambda_q + \frac{1}{2}\,\partial_\nu\,\sigma\right)\sigma^{-1/2}\varphi.$$

By the assumption that $\sigma \equiv 1$ at the boundary we get that indeed $\Lambda_q = \Lambda_\sigma$. Let us note here that if $\sigma \equiv 1$, then $q \equiv 0$.

Now we can use Alessandrini's identity (15) to obtain an equation for the scattering transform by choosing $q_1 = q = \Delta\sqrt{\sigma}\backslash\sqrt{\sigma}$, $v_1 = e^{i\bar{k}\bar{z}}$, $q_2 = 0$ and $v_2 = \psi$, then we get

$$\int_\Omega q(z)e^{i\bar{k}\bar{z}}\psi(z,k)dz = \int_{\partial\Omega} e^{i\bar{k}\bar{z}}(\Lambda_\sigma - \Lambda_1)\psi(z,k)ds.$$

The left hand side is equal to $\mathbf{t}(k)$ by definition and we obtain the representation

$$\mathbf{t}(k) = \int_{\partial\Omega} e^{i\bar{k}\bar{z}}(\Lambda_\sigma - \Lambda_1)\psi(z,k)ds. \tag{16}$$

Now the CGO solutions are involved, so we need an equation for those as well. Using Alessandrini's identity again with $q_1 = 0$, $v_1 = G_k(z-\zeta) = e^{ik(z-\zeta)}g_k(z-\zeta)$, $q_2 = q = \Delta\sqrt{\sigma}\backslash\sqrt{\sigma}$ and $v_2 = \psi$, we obtain

$$\int_\Omega q(\zeta)G_k(z-\zeta)\psi(\zeta,k)d\zeta = \int_{\partial\Omega} G_k(z-\zeta)(\Lambda_1 - \Lambda_\sigma)\psi(\zeta,k)ds(\zeta).$$

This equation can be simplified by using the Lippmann-Schwinger-type equation for ψ (9). By taking the limit $z \to \partial\Omega$, see [57] for details, we obtain the crucial boundary integral equation

$$\psi(z,k)|_{\partial\Omega} = e^{ikz}|_{\partial\Omega} - \int_{\partial\Omega} G_k(z-\zeta)(\Lambda_\sigma - \Lambda_1)\psi(\zeta,k)ds(\zeta). \tag{17}$$

This Fredholm boundary integral equation of the second kind can be solved by knowing the data Λ_σ and the data corresponding to the constant conductivity $\sigma \equiv 1$. This background data can be computed, for instance by simulating the Laplace equation on the given domain. To conclude this section on the inverse conductivity problem, we discuss next a few computational aspects.

2.4 The regularized D-bar algorithm

The D-bar algorithm outlined in the previous section is based on an infinite dimensional operator and the assumption that we can compute the CGO solutions and scattering transform for all parameter $k \in \mathbb{C}\backslash\{0\}$. This is of course not possible in practice. Furthermore, the measured DN map might be contaminated with noise and hence some regularization is needed. In fact the D-bar algorithm as outlined above can be adjusted to be a fully proven regularization strategy for the nonlinear inverse problem [45].

We now present the modifications that are needed to make the algorithm computable. Let us first choose the computational domain for k as the disk $B_0(R) \subset \mathbb{C}$ with radius $R < 0$. We will call R the cut-off radius. Given a noisy DN map, denoted by Λ_σ^δ, then a regularized solution can be obtained by the following algorithm.

The regularized D-bar algorithm

Step 1 For each $k \in B_0(R)\backslash\{0\}$ compute the CGO solutions by solving the boundary integral equation

$$\psi^\delta(z,k)|_{\partial\Omega} = e^{ikz}|_{\partial\Omega} - \int_{\partial\Omega} G_k(z-\zeta)(\Lambda_\sigma^\delta - \Lambda_1)\psi^\delta(\zeta,k)ds(\zeta).$$

Step 2 Evaluate the scattering transform in the computational domain by

$$\mathbf{t}_R^\delta(k) = \begin{cases} \int_{\partial\Omega} e^{i\bar{k}\bar{z}}(\Lambda_\sigma^\delta - \Lambda_1)\psi^\delta(z,k)ds & \text{if } |k| < R, \\ 0 & \text{else.} \end{cases}$$

Step 3 Solve the D-bar equation for each $z \in \Omega$,

$$\overline{\partial}_k \mu_R^\delta(z,k) = \frac{1}{4\pi\bar{k}} \mathbf{t}_R^\delta(k) e_{-k}(z) \overline{\mu_R^\delta(z,k)}.$$

Step 4 Obtain the regularized reconstruction by

$$\sigma^\delta(z) = (\mu_R^\delta(z,0))^2.$$

For details on the implementation of each step, see [51]. In particular, solving the D-bar equation in step 3 can be done by an integral equation

$$\mu_R^\delta(z,k) = 1 + \frac{1}{(2\pi)^2}\int_{B_0(R)} \frac{\mathbf{t}_R^\delta(k')}{(k-k')\bar{k'}} e_{-z}(k')\overline{\mu(z,k')}dk', \tag{18}$$

for fixed $z \in \Omega$. The most notable characteristic of the algorithm above is that it is a proven regularization strategy, see [20] for the definition of a regularization strategy and related analysis. For the sake of clarity we present here a shortened version of the regulariztion result in [45].

Theorem 2.5 (The D-bar algorithm as regularization strategy [45]) *Let $\Omega \subset \mathbb{R}^2$ be the unit disk and the noise level $\delta > 0$ small enough, such that $\|\Lambda_\sigma^\delta - \Lambda_\sigma\|_{H^{1/2}(\partial\Omega)\to H^{-1/2}(\partial\Omega)} < \delta$. The reconstruction operator defined by the above algorithm and denoted by $\mathcal{S}_{R(\delta)}(\Lambda_\sigma^\delta)$, is a well-defined regularization strategy with the cut-off radius satisfying*

$$R(\delta) = -\frac{1}{10}\log\delta.$$

Then the regularized solution satisfies the estimate

$$\|\mathcal{S}_{R(\delta)}(\Lambda_\sigma^\delta) - \sigma\|_{L^\infty(\Omega)} \leq C(-\log\delta)^{-1/14}.$$

A common approximation of the D-bar algorithm is done by omitting step 1 and approximating the CGO solutions by their asymptotic behavior $\psi^{\exp} \approx e^{ikz}$. An approximate scattering transform is then defined by

$$\mathbf{t}^{\exp}(k) := \int_{\partial\Omega} e^{i\bar{k}\bar{z}}(\Lambda_\sigma - \Lambda_1)e^{ikz}ds. \tag{19}$$

This approximation is known as the Born approximation in the D-bar algorithm and is accurate for small $|k|$ as explained in [51], in particular with respect to measurement noise this includes realistic measurement data and hence (19) is a valid approximation even for practical data. Furthermore, the first implementation of the D-bar algorithm used the Born approximation [61] and it was successfully applied to real measurement data [38, 39, 53]. In this shortened form, the D-bar algorithm can be fully parallelized in Step 2-4 and hence is capable of real time imaging [18].

3 The partial boundary problem

The inverse conductivity problem with full-boundary data can be considered as mostly solved and reconstruction algorithms are well studied, hence many researchers

started to investigate the partial-boundary problem in EIT. It was expected to be a rather hard problem to get a grip on theoretically. Furthermore, there are many configurations of boundary data possible, of which not all are of practical relevance, such as different input and measurement domains. In this thesis we concentrate on a realistic setting, that is we are given electrodes that can inject current and measure voltages, and hence we assume that the input and measurement domain coincides. If we assume otherwise, we would make the problem harder than it is. To understand the main difficulty of partial-boundary data we need to introduce the notion of Cauchy data.

Definition 3.1 (Cauchy data set)
Let $\Omega \subset \mathbb{R}^2$ and $u \in H^1(\Omega)$ be a solution of

$$\nabla \cdot \sigma \nabla u = 0, \qquad \text{in } \Omega. \tag{20}$$

The Cauchy data set is defined as

$$\mathcal{C}_\sigma^{\partial\Omega} := \{(u|_{\partial\Omega}, \sigma\, \partial_\nu u|_{\partial\Omega}) \ : \ u \text{ solution of } (20)\}.$$

Shortly explained, the Cauchy data consists of all combinations of Dirichlet and Neumann boundary values for the conductivity equation. It is straightforward to see, that the complete knowledge of the Dirichlet-to-Neumann (DN) map, i.e. for full-boundary data, determines the whole Cauchy data by writing

$$\mathcal{C}_\sigma^{\partial\Omega} = \{(\varphi|_{\partial\Omega}, \Lambda_\sigma \varphi|_{\partial\Omega}) \ : \ \varphi \in H^{1/2}(\partial\Omega)\}.$$

From this knowledge one can obtain as well the Neumann-to-Dirichlet (ND) map. That means in the full-boundary case we can change between the DN and ND maps, up to constants. This is not possible for partial-boundary data, in which case knowing the Dirichlet or Neumann data only on a subset $\Gamma \subset \partial\Omega$ does not determine the full Cauchy data and hence we need to consider these problems separately. In the following we shall discuss both settings and their realization.

3.1 The Dirichlet problem

The partial-boundary Dirichlet problem corresponds to voltages applied on the subset $\Gamma \subset \partial\Omega$. Assuming our domain consists of a noninsulating body (e.g. a human) the applied voltages would immediately distribute to the whole boundary. Thus, there are two cases to consider, either assuming that the voltages are only known on Γ and nonzero elsewhere or to enforce a zero condition on $\Gamma^c = \partial\Omega \setminus \Gamma$. Only the second case

corresponds to a proper partial-boundary problem, given by the following Dirichlet problem

$$\begin{aligned} \nabla \cdot \sigma \nabla u &= 0, \quad \text{in } \Omega, \\ u|_{\partial\Omega} &= g, \quad \text{on } \Gamma \subset \partial\Omega, \\ u|_{\partial\Omega} &= 0, \quad \text{on } \Gamma^c. \end{aligned} \tag{21}$$

This problem is certainly of mathematical interest but only of limited practicality. To realize this setting on a noninsulating body we need to place a separate grounding electrode on Γ^c and measure all potentials with respect to the grounding electrode. Obviously this is not a practical choice, since we could as well just locate proper electrodes at said position. From these complications we can already see that the partial-boundary Dirichlet problem is of limited practical relevance.

Nevertheless, this problem has been studied extensively and many results of mathematical value have been published. These include fairly well understood uniqueness results for different configurations of input and measurement domains and dimension $n \geq 3$ [10, 19, 36, 41, 43]. A thorough survey of these results can be found in [42]. Furthermore, following the tradition, a constructive uniqueness proof has been published by Nachman and Street [55], in this case for dimension $n \geq 3$.

3.2 The Neumann problem

A more practical approach is given by considering the Neumann problem instead. In this case currents are injected to the target and voltages are measured. In particular it is assured that the current is only nonzero at the electrodes and zero elsewhere, hence we can easily realize the Neumann problem given by

$$\begin{aligned} \nabla \cdot \sigma \nabla u &= 0, \quad \text{in } \Omega, \\ \sigma \tfrac{\partial u}{\partial \nu} &= f, \quad \text{on } \Gamma \subset \partial\Omega, \\ \sigma \tfrac{\partial u}{\partial \nu} &= 0, \quad \text{on } \Gamma^c, \end{aligned} \tag{22}$$

with ν denoting the outward normal. The biggest obstacle of this setting is that the resulting voltages are in general still supported on the whole boundary and hence ideally we would need to measure on the full boundary, which of course does not make sense if we only apply currents on the partial boundary. That means we can only expect to know the voltages on the input and measurement domain and we need to extrapolate from this information. Possibilities for this extrapolation are discussed in Publication II and IV of this thesis.

For the Neumann problem there are fewer theoretical results, especially the uniqueness question has not been answered thourougly yet. Results exist in particular for C^2 conductivities; for the case of coinciding measurement and input domains

in $\mathbb{R}^2$ by [37], in higher dimensions in [29], and for different input and measurement domains in [16]. A more pratical case with bisweep data has been addressed in [33]. These results are of great importance for the theoretical understanding, but are so far not readily applicable for the computational reconstruction task. For instance, given only (very limited) finite data uniqueness can not be guaranteed any more, as demonstrated for the point electrode model in [15]. To conclude this chapter we will shortly discuss a few computational approaches for partial data.

3.3 Reconstruction algorithms for partial-boundary data

Reconstruction algorithms can be roughly divided into two classes: direct and indirect methods. Algorithms based on direct inversion are closely related to theoretical studies and demand a deep understanding of the mathematical structure of the problem. An investigation on direct inversion from partial-boundary data has been done in [26] based on the D-bar method by utilizing localized basis functions (Haar wavelets) to recover the complex geometric optics (CGO) solutions. Other direct approaches that can be used for partial data are for instance, complex spherical probing with localized boundary measurements [34, 35] and monotonicity based methods [27, 28].

On the other side, indirect approaches for the partial-boundary problem are more common and perform very well in reconstruction quality, but tend to be slow. Typically those approaches consist in minimizing a carefully chosen penalty functional, which is based on a thorough understanding of physical aspects of the imaged target. In this category there are many algorithms available. We mention a few that are of importance in our perception. Those include reconstruction algorithms based on sparsity priors for simulated continuum data [22] and planar real measurements [23]. Algorithms based on the complete electrode model [14, 62], which takes contact impedances at the electrodes into account, include domain truncation approaches [12, 13, 49], difference imaging [48], and electrode configurations that cover only a certain part of the boundary [50, 65].

4 Measurement models

In this section we will shortly discuss the different measurement models, i.e. the continuum model and electrode models, and how we can represent the ND (or DN) map for the reconstruction task from the collected data.

4.1 Continuum model

In the continuum model we assume to know the boundary value as a function on the whole boundary. Typically the Neumann problem is simulated due to stability reasons of the forward problem [51], but as we have discussed in Section 3 we can obtain the DN map from this measurement in case of full-boundary data. That means the boundary value problem with Neumann data $\varphi \in H^{-1/2}(\partial\Omega)$ as follows is simulated

$$\begin{aligned} \nabla \cdot \sigma \nabla u &= 0, && \text{in } \Omega, \\ \sigma\, \partial_\nu u &= \varphi, && \text{on } \partial\Omega, \end{aligned} \tag{23}$$

and the solution on the boundary $u|_{\partial\Omega} \in H^{1/2}(\partial\Omega)$ is recorded. For uniqueness we assume that the solutions u satisfy $\int_{\partial\Omega} u \; ds = 0$ and due to conservation of charge $\int_{\partial\Omega} \varphi \; ds = 0$. Consequently we are measuring the ND map. For the reconstruction algorithms we need a matrix representation, which can be obtained by first choosing an orthonormal basis of $L^2(\partial\Omega)$. For instance, let Ω be the unit disk and we choose the orthonormal basis given by the Fourier basis functions $\varphi_n(\theta) = \frac{1}{\sqrt{2\pi}} e^{in\theta}$ for $n \in \mathbb{Z}\backslash\{0\}$. Now we can obtain a matrix approximation $\mathbf{R}_\sigma$ of the ND map from the measurements $\mathcal{R}_\sigma \varphi_n = u_n|_{\partial\Omega}$ with respect to the orthonormal basis as

$$(\mathbf{R}_\sigma)_{n,\ell} = (\mathcal{R}_\sigma \varphi_n, \varphi_\ell)_{L^2(\partial\Omega)} = \frac{1}{\sqrt{2\pi}} \int_{\partial\Omega} u_n|_{\partial\Omega}(\theta) e^{-i\ell\theta} d\theta.$$

Having a matrix representation of the ND map, we can simply invert it to obtain the matrix approximation for the DN map that is used in the D-bar algorithm as described in Section 2. In case we have only partial-boundary data, we can not simply invert the ND matrix, and hence the D-bar algorithm needs to be reformulated for ND maps, as done in Publication II of this thesis.

4.2 Electrode models

In real life applications we can not expect to measure a function on the whole boundary and hence we need to consider proper electrode models. The simplest model is the so-called gap model and approximates currents and voltages by a constant on each electrode. In particular, given M electrodes $E_1, \ldots, E_M$ then each electrode is assigned a current value J_m. The voltages are assumed to have the values measured at the center of each electrode $U_m = u(\text{center of } E_m)$. Together the gap model can be written as

$$\begin{aligned} \nabla \cdot \sigma \nabla u &= 0, && \text{in } \Omega, \\ \sigma\, \partial_\nu u &= J_m, && \text{on } E_m,\ m = 1, \ldots, M, \\ \sigma\, \partial_\nu u &= 0, && \text{otherwise.} \end{aligned} \tag{24}$$

Similar to (23) we require the zero mean conditions $\sum_m U_m = 0$ and $\sum_m J_m = 0$. A typical choice for the boundary condition is given by trigonometric basis functions. Assuming we have M equally spaced electrodes with center $\theta_m = 2\pi m/M$. Then we are able to obtain $M-1$ linearly independent basis vectors $J^n \in \mathbb{R}^M$, for $n = 1, \ldots, M-1$. The values on each electrode, based on the trigonometric current pattern, are given by

$$J_m^n = \frac{\sqrt{2}}{\sqrt{M}} \begin{cases} \cos(n \cdot \theta_m) & \text{for } n < M/2, \\ \frac{1}{\sqrt{2}} \cos((M/2) \cdot \theta_m) & \text{for } n = M/2, \\ \sin((M-n) \cdot \theta_m) & \text{for } n > M/2. \end{cases}$$

The gap model is in fact in many cases sufficiently accurate to model real measurements as has been demonstrated for instance in [38, 39]. A matrix approximation of the ND map can be obtained by taking the inner products of the measurement $U^n \in \mathbb{R}^M$ and the current vectors as

$$(\mathbf{R}_\sigma^{\text{gap}})_{n,\ell} = (U^n, J^\ell)_2.$$

Nevertheless, the gap model is not entirely realistic and not sufficient for simulating the measurement process, hence for building an iterative method with a forward solver we need a better model. The first improvement to get a better approximation is done by the assumption that the current is not constant over the electrode and rather that the applied current equals the integral over each electrode, that is

$$J_m = \frac{1}{|E_m|} \int_{E_m} \sigma \, \partial_\nu \, u ds.$$

To model real measurement data most accurately we also need to take a phenomena known as contact impedances into account. This is done to model the electrochemical effect of a thin resistive layer forming between the electrodes and the measured target, this is incorporated by a Robin boundary condition to the system. The full model, known as the *complete electrode model* (CEM), is then given by

$$\begin{aligned} \nabla \cdot \sigma \nabla u &= 0 \text{ in } \Omega, \\ \sigma \, \partial_\nu \, u &= 0 \text{ on } \partial\Omega \backslash \Gamma \\ u + z\sigma \, \partial_\nu \, u &= U \text{ on } \Gamma \\ \tfrac{1}{|E_m|} \textstyle\int_{E_m} \sigma \, \partial_\nu \, u &= J_m \text{ for } 1 \le m \le M, \end{aligned} \tag{25}$$

equipped with the same zero mean conditions as in the gap model. This model has been first discussed by [14] and well-posedness has been shown in [62]. For

the definition of the measurement operator it is useful to define spaces of piecewise constant functions on the electrodes by

$$T(\partial\Omega) := \left\{ V \in L^2(\partial\Omega) \,\middle|\, \sum_{m=1}^{M} \chi_m V_m,\ V_m \in \mathbb{R}, \text{ and } V = 0 \text{ on } \Gamma^c \right\}.$$

It clearly follows that $T(\partial\Omega) \subset L^2(\partial\Omega)$ and we denote $T_\diamond(\partial\Omega) = T(\partial\Omega) \cap L^2_\diamond(\partial\Omega)$, where $L^2_\diamond(\partial\Omega)$ denotes L^2 functions with zero mean. The corresponding measurement operator for the CEM can then be defined as the mapping

$$\mathcal{R}^E_\sigma : J \mapsto U, \quad T_\diamond(\partial\Omega) \to T(\partial\Omega).$$

This operator is linear and continuous as discussed in [31, 32]. The matrix approximation of the measurement operator can be obtained similarly to the gap model, but we need to substract the contact impedance times input current from the measurement, such that

$$(\mathbf{R}^{\mathrm{CEM}}_\sigma)_{n,\ell} = (U^n - zJ^n, J^\ell)_2.$$

In case we do not know the contact impedance, the computation of $\mathbf{R}^{\mathrm{CEM}}_\sigma$ can only done with an additional error. Nevertheless, if we assume that the contact impedance does not change between measurements, then taking the difference of measured currents approximately cancels the contact impedance term and a difference ND matrix can be approximated by

$$(\mathbf{R}^{\mathrm{CEM}}_{\sigma_1,\sigma_2})_{n,\ell} = (U^n_{\sigma_1} - U^n_{\sigma_2}, J^\ell)_2.$$

Especially for the standard D-bar algorithm the case $\sigma_2 \equiv 1$ is of special interest.

5 Discussion of results

5.1 Publication I

We introduce two main ideas for improving EIT images obtained with the D-bar algorithm. Firstly we propose a new data fidelity term directly derived from the nonlinear inversion process, by utilizing the CGO solutions. The second idea is to post-process the reconstructions obtained with tools from image processing. In particular we are interested in algorithms for image segmentation, as in [25]. A particular approach has been proposed by Mumford and Shah in 1985 for detecting

boundaries in general images [52]. Given an initial (corrupted) image $\widetilde{u}$, we obtain an edge-preserving approximation as the minimizer of

$$E_{MS}(u,K) = \int_{\Omega\setminus K} |\nabla u|^2 dx + \beta \int_{\Omega} (u-\widetilde{u})^2 dx + \alpha |K|, \tag{26}$$

where K denotes a curve segmenting Ω, $|K|$ the length of K, and the two parameters $\alpha, \beta > 0$ are used for weighting the terms. The idea is to find the minimum of $E_{MS}(u,K)$ over images u and curves K; the minimizing image can then be considered as a piecewise constant segmented version of $\widetilde{u}$.

As K is unknown and singular, numerically minimizing (26) is a challenging task; in particular formulating a gradient-descent method with respect to K is not straightforward. Thus, numerical studies mostly concentrate on finding an approximation to (26). The approach we take in this publication is to use an elliptic approximation introduced by Ambrosio and Tortorelli [4]. Their idea can be summarized as introducing an edge-strength function $v : \Omega \to [0,1]$ that controls the gradient of u. The Ambrosio-Tortorelli (AT) functional is then defined by

$$E_{AT}(u,v) = \int_{\Omega} \beta(u-\widetilde{u})^2 + v^2|\nabla u|^2 + \alpha\left(\rho|\nabla v|^2 + \frac{(1-v)^2}{4\rho}\right) dx. \tag{27}$$

The additional parameter $\rho > 0$ specifies, roughly speaking, the edge width of u. The advantage of (27) over (26) is that the minimizer can be obtained by an artificial time evolution formulated via a coupled PDE as the gradient-descent equations with an imposed homogeneous Neumann boundary condition. These equations can be easily solved and used to compute a minimizer.

We then propose to evaluate the iteratively obtained images from minimizing (27) with the concept of the CGO sinogram. The CGO sinogram is defined for the CGO solution $\mu(z,k) = e^{-ikz}\psi(z,k)$, as described in Definition 2.1. We remind that the functions μ satisfy the asymptotic condition $\mu(z,k) - 1 \in W^{1,p}(\mathbb{R}^2)$. Following this we defined the CGO sinogram as

$$\begin{aligned} \mathcal{S}_\sigma(\theta,\varphi,r) :=& \mu(e^{i\theta}, re^{i\varphi}) - 1 \\ =& \exp(-ire^{i(\varphi+\theta)})\,\psi(e^{i\theta}, re^{i\varphi}) - 1. \end{aligned} \tag{28}$$

The CGO sinogram can be calculated from the measurement data, i.e. the DN map, as well as for smooth images directly from the Lippmann-Schwinger type equation (7). It is demonstrated in the paper that the CGO sinogram clearly encodes some geometric properties, which can be used for evaluating the reconstructions.

The basic idea of the proposed algorithm can be summarized as follows: given a measured DN map, reconstruct an initial blurry D-bar reconstruction and deblur this image iteratively by solving (27). Whether the newly obtained image is better or not can be verified by evaluating the error of CGO sinograms corresponding to the measured DN map and the new iterate.

It is demonstrated that this procedure is capable of significantly sharpening D-bar reconstructions obtained from continuum EIT data. Additionally, we can assure that the sharpened images are an improvement and reduce the error to the true conductivity, by utilizing the nonlinear information contained in the CGO solutions.

5.2 Publication II

The D-bar algorithm has been formulated for full-boundary continuum data and hence, in theory, has limited applications. Nevertheless, it has been successfully applied to real data obtained from electrodes and the convergence results for noisy data in [44, 45] have established the D-bar algorithm as full nonlinear regularization strategy. Going one step further, this publication investigates the possibility to apply the classical D-bar algorithm to data that is only collected on part of the boundary. The biggest obstacle is given by the fact that the Neumann and Dirichlet problems are not (essentially) equivalent any more, as discussed in Section 3, and hence we can not obtain the DN map by inverting the ND map. Due to this restriction we have reformulated the D-bar algorithm to work directly with the obtained ND maps. This is essentially done by stating Alessandrini's identity for ND maps and then deriving the equations for the scattering transform and CGO solutions for ND maps. Nevertheless, the obtained equations are not sufficient to formulate a full nonlinear inversion algorithm, since the CGO solutions, given by

$$\psi(z,k) = e^{ikz} - (B_k - \frac{1}{2})(\mathcal{R}_1 - \mathcal{R}_\sigma)\,\partial_\nu\,\psi(\cdot,k),$$

are dependend on their normal derivative and can not be readily computed as such. One could formulate a proper boundary integral equation with the normal derivative of ψ on both sides as done in [40], but this leads to further numerical problems that we wanted to avoid. A similar problem arises in the calculation of the scattering transform

$$\mathbf{t}(k) = \int_{\partial\Omega} \left(\partial_\nu\, e^{i\bar{k}\bar{\zeta}}\right)(\mathcal{R}_1 - \mathcal{R}_\sigma)\,\partial_\nu\,\psi(\zeta,k)ds(\zeta),$$

where the normal derivative is needed. Thus, we rather propose to calculate an approximation of the CGO solutions and the scattering transform by setting the

normal derivative of ψ equal to its asymptotic behaviour

$$\partial_\nu \psi(k, z) \approx \partial_\nu e^{ikz}.$$

This approach is related to the classical Born approximation as initially proposed in [61] and discussed in Section 2.4. The approximate CGO solutions are not needed for the reconstruction task itself, but can be used to calculate the CGO sinogram for instance. Furthermore, new developments have shown that one can formulate an algorithm for edge detection based on the knowledge of the CGO solutions [24].

At last the publication establishes a convergence result for the data error of partial-boundary to full-boundary data, as well as for the resulting reconstructions. In particular it is shown in Proposition 3.2 and Theorem 4.3, that the error in data and reconstruction depends linearly on the domain that is missing. It is demonstrated in numerical experiments that the convergence results hold for simulated data. Reconstructions are then presented for the unit disk as well as for a chest shaped phantom.

5.3 Publication III

The majority of iterative reconstruction algorithms for EIT rely on some prior information of the target. Either the simple assumption that the conductivity is piecewise constant or more thorough knowledge on the structure of the imaged object. The missing possibility of incorporating such prior knowledge to the D-bar algorithm has been a major drawback that has been fixed by recent advances due to [2, 3]. The basic idea is to utilize known structures of the imaged object and to incorporate them as information in the scattering transform for the reconstruction task. To motivate the approach, let us assume one wants to do a respiratory function test of a human. Then the approximate shapes, sizes, and locations of organ boundaries may be obtained from a previous CT or ultrasound scan, or by consulting an anatomical atlas. As described in the publication we can compute a scattering transform directly from such prior information that can be used in the reconstruction process in two essential steps.

The first step is to fill in bad parts of the scattering transform obtained from partial-boundary measurements. For partial data the scattering data tends to blow up in a noncircular manner and hence leads to severe instabilities in the reconstruction. In addition noise will blow up the scattering data for large values of $|k|$. Consequently, one can extend the scattering transform outside the stable region with the scattering data of the prior.

The second crucial step is given by adjusting the integral equation (18) for solving the D-bar equation. In fact, (18) is the limiting case of

$$\mu(z,k) = \lim_{R\to\infty} \left\{ \frac{1}{\pi R^2} \int_{|k|\le R} \mu(z,k)dk \right. \\ \left. + \frac{1}{(2\pi)^2} \int_{|k|\le R} \frac{\mathbf{t}(k')}{(k-k')\bar{k}'} e_{-z}(k')\overline{\mu(z,k')}dk' \right\}.$$

Instead of replacing the first integral by its limit 1, we can use the scattering transform $\mu^{\mathbf{PR}}$ computed from the prior for a given cut-off radius R_2 and set

$$\mu^{\text{int}}(z) := \frac{1}{\pi R_2^2} \int_{|k|\le R_2} \mu^{\mathbf{PR}}(z,k)dk.$$

This way we may incorporate the a priori knowledge into the reconstruction. For a thourough introduction of the prior method we refer to [2, 3]. The publication in this thesis examines the effectiveness of the prior approach for the detection of pathologies form partial-boundary electrode data. It is important to note that for computing the prior no pathologies were assumed.

5.4 Publication IV

As discussed in the previous publications, restricting the input currents to a part of the boundary will lead to differences in the measured data to the ideal continuum case. Even if one just considers an electrode setting, the collected data will be inherently different. This publication examines the possibility to recover information of the ideal full-boundary data by utilizing the knowledge of projections applied to produce the input currents. In this context, recovering information of full-boundary data is understood as computing an approximation to the ND matrix by formulating an optimization problem on the coefficients with respect to the orthonormal basis of applied currents. The desired approximation can then be computed by solving a simple matrix-vector equation.

The publication investigates a realistic setting in which the amount and size of electrodes is fixed. A main question is, if the approximation procedure can be applied to measurements from the *complete electrode model* (CEM). For this purpose we introduce the so-called *electrode continuum model* (ECM) that involves the partial ND map and is more suitable to interpret real measurements in the continuum setting. In Theorem 2.2 it is shown, that the approximation error of the ECM to the CEM for partial boundary measurements depends linearly on the length of the electrodes,

but is independent of the missing boundary. This approximation result is related to the study in [31, 32], where the author analyzed the approximation properties of the complete electrode model to the ideal continuum model.

An auxiliary result in the publication states that the coefficients of the ND matrix for rotationally symmetric conductivities can be recovered from one single injected current pattern. The proposed approximation procedure is successfully applied to simulated ECM and CEM data, as well as real measured data from the KIT4 system located at the University of Eastern Finland, Kuopio [30, 47].

References

[1] G. Alessandrini, *Stable determination of conductivity by boundary measurements*, Applicable Analysis, 27 (1988), pp. 153–172.

[2] M. Alsaker, *Computational advancements in the D-bar reconstruction method for 2-D electrical impedance tomography*, PhD thesis, Colorado State University. Libraries, 2016.

[3] M. Alsaker and J. L. Mueller, *A D-bar algorithm with a priori information for 2-D Electrical Impedance Tomography*, SIAM J. on Imaging Sciences, 9 (2016), pp. 1619–1654.

[4] L. Ambrosio and V. M. Tortorelli, *Approximation of functionals depending on jumps by elliptic functionals via* Γ*-convergence*, Communications on Pure and Applied Mathematics, 43 (1990), pp. 999–1036.

[5] K. Astala and L. Päivärinta, *A boundary integral equation for Calderón's inverse conductivity problem*, in Proc. 7th Internat. Conference on Harmonic Analysis, Collectanea Mathematica, 2006.

[6] J. A. Barceló, T. Barceló, and A. Ruiz, *Stability of the inverse conductivity problem in the plane for less regular conductivities*, Journal of Differential Equations, 173 (2001), pp. 231–270.

[7] R. Beals and R. R. Coifman, *Multidimensional inverse scatterings and nonlinear partial differential equations*, in Pseudodifferential operators and applications (Notre Dame, Ind., 1984), Amer. Math. Soc., Providence, RI, 1985, pp. 45–70.

[8] M. Boiti, J. P. Leon, M. Manna, and F. Pempinelli, *On a spectral transform of a KdV-like equation related to the Schrödinger operator in the plane*, Inverse Problems, 3 (1987), pp. 25–36.

[9] R. M. Brown and G. Uhlmann, *Uniqueness in the inverse conductivity problem for nonsmooth conductivities in two dimensions*, Communications in Partial Differential Equations, 22 (1997), pp. 1009–1027.

[10] A. L. Bukhgeim and G. Uhlmann, *Recovering a potential from partial Cauchy data*, Communications in Partial Differential Equations, 27 (2002), pp. 653–668.

[11] A.-P. Calderón, *On an inverse boundary value problem*, in Seminar on Numerical Analysis and its Applications to Continuum Physics (Rio de Janeiro, 1980), Soc. Brasil. Mat., Rio de Janeiro, 1980, pp. 65–73.

[12] D. Calvetti, P. J. Hadwin, J. M. Huttunen, D. Isaacson, J. P. Kaipio, D. McGivney, E. Somersalo, and J. Volzer, *Artificial boundary conditions and domain truncation in electrical impedance tomography. part i: Theory and preliminary results*, Inverse Problems & Imaging, 9 (2015), pp. 749–766.

[13] D. Calvetti, P. J. Hadwin, J. M. Huttunen, J. P. Kaipio, and E. Somersalo, *Artificial boundary conditions and domain truncation in electrical impedance tomography. part ii: Stochastic extension of the boundary map.*, Inverse Problems & Imaging, 9 (2015), pp. 767–789.

[14] K. Cheng, D. Isaacson, J. Newell, and D. Gisser, *Electrode models for electric current computed tomography*, IEEE Transactions on Biomedical Engineering, 36 (1989), pp. 918–924.

[15] L. Chesnel, N. Hyvönen, and S. Staboulis, *Construction of indistinguishable conductivity perturbations for the point electrode model in electrical impedance tomography*, SIAM Journal on Applied Mathematics, 75 (2015), pp. 2093–2109.

[16] F. J. Chung, *Partial data for the neumann-to-dirichlet map*, Journal of Fourier Analysis and Applications, 21 (2015), pp. 628–665.

[17] A. M. Cormack and G. N. Hounsfield, *The nobel prize in physiology or medicine*, 1979.

[18] M. Dodd and J. L. Mueller, *A real-time D-bar algorithm for 2-D electrical impedance tomography data*, Inverse problems and imaging, 8 (2014), pp. 1013–1031.

[19] D. Dos Santos Ferreira, C. E. Kenig, J. Sjöstrand, and G. Uhlmann, *Determining a magnetic Schrödinger operator from partial Cauchy data*, Communications in mathematical physics, 271 (2007), pp. 467–488.

[20] H. Engl, M. Hanke, and A. Neubauer, *Regularization of inverse problems*, Kluwer Academic Publishers, 1996.

[21] L. D. Faddeev, *Increasing solutions of the Schrödinger equation*, Soviet Physics Doklady, 10 (1966), pp. 1033–1035.

[22] H. Garde and K. Knudsen, *Sparsity prior for electrical impedance tomography with partial data*, Inverse Problems in Science and Engineering, DOI: 10.1080/17415977.2015.1047365 (2015), pp. 1–18.

[23] M. Gehre, T. Kluth, C. Sebu, and P. Maass, *Sparse 3D reconstructions in electrical impedance tomography using real data*, Inverse Problems in Science and Engineering, 22 (2014), pp. 31–44.

[24] A. Greenleaf, M. Lassas, M. Santacesaria, S. Siltanen, and G. Uhlmann, *Propagation and recovery of singularities in the inverse conductivity problem*, arXiv:1610.01721, (2016).

[25] S. Hamilton, J. M. Reyes, S. Siltanen, and X. Zhang, *A hybrid segmentation and d-bar method for electrical impedance tomography*, SIAM Journal on Imaging Sciences, 9 (2016), pp. 770–793.

[26] S. J. Hamilton, M. Lassas, and S. Siltanen, *A Direct Reconstruction Method for Anisotropic Electrical Impedance Tomography*, Inverse Problems, 30:(075007) (2014).

[27] B. Harrach and M. Ullrich, *Monotonicity-based shape reconstruction in electrical impedance tomography*, SIAM Journal on Mathematical Analysis, 45 (2013), pp. 3382–3403.

[28] ——, *Resolution guarantees in electrical impedance tomography*, IEEE transactions on medical imaging, 34 (2015), pp. 1513–1521.

[29] ——, *Local uniqueness for an inverse boundary value problem with partial data*, in Proc. Amer. Math. Soc (accepted for publication), 2016.

[30] A. Hauptmann, V. Kolehmainen, N. M. Mach, T. Savolainen, A. Seppänen, and S. Siltanen, *Open 2d electrical impedance tomography data archive*, arXiv:1704.01178, (2017).

[31] N. Hyvönen, *Complete electrode model of electrical impedance tomography: Approximation properties and characterization of inclusions*, SIAM Journal on Applied Mathematics, 64 (2004), pp. 902–931.

[32] N. Hyvönen, *Approximating idealized boundary data of electric impedance tomography by electrode measurements*, Mathematical Models and Methods in Applied Sciences, 19 (2009), pp. 1185–1202.

[33] N. Hyvönen, P. Piiroinen, and O. Seiskari, *Point measurements for a neumann-to-dirichlet map and the calderón problem in the plane*, SIAM Journal on Mathematical Analysis, 44 (2012), pp. 3526–3536.

[34] T. Ide, H. Isozaki, S. Nakata, and S. Siltanen, *Local detection of three-dimensional inclusions in electrical impedance tomography*, Inverse problems, 26 (2010), p. 035001.

[35] T. Ide, H. Isozaki, S. Nakata, S. Siltanen, and G. Uhlmann, *Probing for electrical inclusions with complex spherical waves*, Communications on pure and applied mathematics, 60 (2007), pp. 1415–1442.

[36] O. Imanuvilov, G. Uhlmann, and M. Yamamoto, *The Calderón problem with partial data in two dimensions*, American Mathematical Society, 23 (2010), pp. 655–691.

[37] O. Imanuvilov, G. Uhlmann, and M. Yamamoto, *Inverse boundary value problem by partial data for the neumann-to-dirichlet-map in two dimensions*, arXiv preprint arXiv:1210.1255, (2012).

[38] D. Isaacson, J. Mueller, J. Newell, and S. Siltanen, *Imaging cardiac activity by the D-bar method for electrical impedance tomography*, Physiological Measurement, 27 (2006), pp. S43–S50.

[39] D. Isaacson, J. L. Mueller, J. C. Newell, and S. Siltanen, *Reconstructions of chest phantoms by the D-bar method for electrical impedance tomography*, IEEE Transactions on Medical Imaging, 23 (2004), pp. 821–828.

[40] M. Isaev and R. Novikov, *Reconstruction of a potential from the impedance boundary map*, Eurasian Journal of Mathematical and Computer Applications, 1 (2013), pp. 5–28.

[41] V. Isakov, *On uniqueness in the inverse conductivity problem with local data*, Inverse Problems and Imaging, 1 (2007), pp. 95–105.

[42] C. Kenig and M. Salo, *Recent progress in the Calderón problem with partial data*, Contemp. Math, 615 (2014), pp. 193–222.

[43] C. Kenig, J. Sjostrand, and G. Uhlmann, *The Calderón problem with partial data*, Annals of Mathematics-Second Series, 165 (2007), pp. 567–592.

[44] K. Knudsen, M. Lassas, J. Mueller, and S. Siltanen, *D-bar method for electrical impedance tomography with discontinuous conductivities*, SIAM Journal on Applied Mathematics, 67 (2007), p. 893.

[45] K. Knudsen, M. Lassas, J. Mueller, and S. Siltanen, *Regularized D-bar method for the inverse conductivity problem*, Inverse Problems and Imaging, 3 (2009), pp. 599–624.

[46] K. Knudsen and A. Tamasan, *Reconstruction of less regular conductivities in the plane*, Communications in Partial Differential Equations, 29 (2004), pp. 361–381.

[47] J. Kourunen, T. Savolainen, A. Lehikoinen, M. Vauhkonen, and L. Heikkinen, *Suitability of a pxi platform for an electrical impedance tomography system*, Measurement Science and Technology, 20 (2008), p. 015503.

[48] D. Liu, V. Kolehmainen, S. Siltanen, A.-m. Laukkanen, and A. Seppänen, *Estimation of conductivity changes in a region of interest with electrical impedance tomography*, Inverse Problems and Imaging, 9 (2015), pp. 211–229.

[49] D. Liu, V. Kolehmainen, S. Siltanen, and A. Seppänen, *A nonlinear approach to difference imaging in EIT; assessment of the robustness in the presence of modelling errors*, Inverse Problems, 31 (2015), p. 035012.

[50] J. Mueller, D. Isaacson, and J. C. Newell, *A reconstruction algorithm for electrical impedance tomography data collected on rectangular electrode arrays*, IEEE Transactions on Biomedical Engineering, 49 (1999), pp. 1379–1386.

[51] J. Mueller and S. Siltanen, *Linear and Nonlinear Inverse Problems with Practical Applications*, vol. 10 of Computational Science and Engineering, SIAM, 2012.

[52] D. Mumford and J. Shah, *Boundary detection by minimizing functionals*, in IEEE Conference on Computer Vision and Pattern Recognition, 1985.

[53] E. Murphy, *2-D D-bar Conductivity Reconstructions on Non-circular Domains*, PhD thesis, Colorado State University, Fort Collins, CO, 2007.

[54] A. Nachman and M. J. Ablowitz, *A multi-dimensional inverse scattering method*, Studies in Applied Mathematics, 71 (1984), p. 243.

[55] A. Nachman and B. Street, *Reconstruction in the Calderón problem with partial data*, Communications in Partial Differential Equations, 35 (2010), pp. 375–390.

[56] A. I. Nachman, *Reconstructions from boundary measurements*, Annals of Mathematics, 128 (1988), pp. 531–576.

[57] ——, *Global uniqueness for a two-dimensional inverse boundary value problem*, Annals of Mathematics, 143 (1996), pp. 71–96.

[58] R. Novikov, *A multidimensional inverse spectral problem for the equation* $-\delta\psi+(v(x)-eu(x))\psi=0$, Functional Analysis and Its Applications, 22 (1988), pp. 263–272.

[59] J. Radon, *über die Bestimmung von Funktionen durch ihre Integralwerte längs gewisser Mannigfaltigkeiten*, Berichte über die Verhandlungen der Sächsischen Akademien der Wissenschaften, Leipzig. Mathematisch-physische Klasse, 69 (1917), pp. 262–267.

[60] S. Siltanen, *Electrical impedance tomography and Faddeev Green's functions*, Annales Academiae Scientiarum Fennicae Mathematica Dissertationes, 121 (1999), p. 56. Dissertation, Helsinki University of Technology, Espoo, 1999.

[61] S. Siltanen, J. Mueller, and D. Isaacson, *An implementation of the reconstruction algorithm of A. Nachman for the 2-D inverse conductivity problem*, Inverse Problems, 16 (2000), pp. 681–699.

[62] E. Somersalo, M. Cheney, and D. Isaacson, *Existence and uniqueness for electrode models for electric current computed tomography*, SIAM Journal on Applied Mathematics, 52 (1992), pp. 1023–1040.

[63] J. Sylvester and G. Uhlmann, *A uniqueness theorem for an inverse boundary value problem in electrical prospection*, Communications on Pure and Applied Mathematics, 39 (1986), pp. 91–112.

[64] J. Sylvester and G. Uhlmann, *A global uniqueness theorem for an inverse boundary value problem*, Annals of Mathematics, 125 (1987), pp. 153–169.

[65] P. J. Vauhkonen, M. Vauhkonen, T. Savolainen, and J. P. Kaipio, *Three-dimensional electrical impedance tomography based on the complete electrode model*, IEEE Transactions on Biomedical Engineering, 46 (1999), pp. 1150–1160.